ACS OMEGA

Open Access

http://pubs.acs.org/journal/acsodf

Article

Adsorption Properties of Natural Zeolite Supported by Chitosan on Cd(II) in Micropolluted Irrigation Water

Yan Shi,* Xin Wang, Changping Feng, Weiwei Chen, and Shipeng Yang

Cite This: *ACS Omega* 2024, 9, 573−584

Read Online

ACCESS | Metrics & More | Article Recommendations | Supporting Information

ABSTRACT: This study utilized a 1% chitosan solution (dissolved in 2% acetic acid), with a chitosan-to-zeolite mass ratio of 0.005, to successfully prepare chitosan-loaded natural zeolite. The performance of chitosan-modified natural zeolite in the removal of low-concentration cadmium ions in the presence of micropollutants was investigated. The adsorbent was characterized using X-ray diffraction (XRD), Fourier transform infrared (FTIR), and scanning electron microscopy (SEM)/energy-dispersive spectroscopy (EDS) techniques. The impact of modified adsorbent dosage, pH value, contact time, temperature, and initial concentration on adsorption performance was discussed. Additionally, the adsorption kinetics, isotherms, and thermodynamics of cadmium on chitosan-modified zeolites were analyzed. The results indicated that the modified zeolite exhibited a dispersed and porous structure with increased surface area, average pore size, and total pore volume. Under the conditions of 25 °C, pH 6, a dosage of 8 g/L, and a 60 min adsorption reaction time, chitosan-loaded natural zeolite (CNZ) achieved a removal efficiency of over 94.51% for a 100 μg/L cadmium solution (in a 100 mL volume). The adsorption process followed the Langmuir model, suggesting monolayer adsorption. The adsorption kinetics followed a pseudo-second-order equation, indicating an exothermic process with an increase in entropy. Chitosan-loaded natural zeolite demonstrated improved adsorption capacity and effectively removed cadmium from water contaminated with micropollutants.

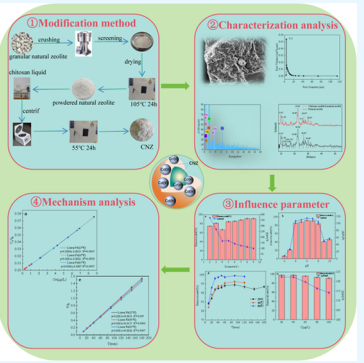

1. INTRODUCTION

China is one of the origins of world agriculture with a rich agricultural history. Additionally, it is among the countries facing some of the most severe challenges in terms of population, resources, and the environment.[1] Confronted with a significant shortage of water resources, China's agricultural development is constrained by a scarcity of water for agricultural use. Treated wastewater has been widely employed as a critical alternative water resource for irrigating farmlands.[2] However, wastewater also contains heavy metals, and improper wastewater irrigation practices can pose hazards to soil, groundwater, and crop quality. According to the 2015 National Soil Survey in China, 19.4% of agricultural soils in China are affected by heavy metal pollution, underscoring the urgency of addressing soil contamination resulting from wastewater irrigation.[3] Among these heavy metal pollutants, cadmium is a key focus, and its pollution has impacted 12 000 ha of farmland.[4,5] Cadmium also stands out as a prime example of exceeding permissible levels in China's agricultural products.[6] Zhu and others conducted an investigation into major food sources in rural southern China, such as rice and vegetables, revealing median cadmium concentrations of 0.33 and 0.08 mg per kilogram, respectively. The cadmium content in rice and vegetable samples exceeded Chinese health standards by 65.31 and 23.75%, respectively.[7] As a nonessential trace element, cadmium ranks among the most potent heavy metals in terms of biological toxicity. Upon root absorption, cadmium can severely harm plants and, through the food chain, ultimately threaten human health, causing damage to bones, kidneys, nerves, and other areas.[8,9] Enhancing treatment techniques for heavy metal pollutants in slightly contaminated irrigation water and achieving the secure agricultural utilization of farmland tainted with heavy metals hold paramount importance. This effort not only contributes to maintaining social stability and improving the ecological environment but also enhances the competitiveness of agricultural products.[10]

Currently, there are various methods available for the treatment of wastewater containing heavy metal pollutants, such as membrane separation,[11−15] ion exchange,[16,17] electrochemical treatment,[18−20] chemical precipitation,[21−23] oxidation−reduction methods, adsorption, phytoremediation, etc. Among these methods, adsorption is considered the most effective due to its low cost, high efficiency, easy availability of adsorbents, simplicity of operation, and minimal secondary pollution.[24,25] Therefore, the development of highly efficient, low-cost, and environmentally friendly adsorbents has become an important direction of research for scholars both domestically and internationally.

Received: August 21, 2023
Revised: December 14, 2023
Accepted: December 15, 2023
Published: December 27, 2023

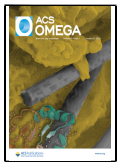

Many researchers have studied the use of natural or synthetic zeolites, industrial waste materials,[26] agricultural byproducts,[27] clay minerals, and other materials as adsorbents. Zeolites are a group of hydrated aluminosilicate minerals with a unique crystal structure containing numerous cavities and channels internally. They have a large specific surface area and exhibit excellent properties and environmental attributes, such as strong adsorption and ion exchange capabilities. China has abundant natural zeolite reserves, estimated at 4 billion tons, ranking among the top in the world with an annual production capacity of 8 million tons.[28] However, natural zeolites have some limitations, such as easily clogged pores, poor interconnectivity between pores, and small pore sizes, which result in less effective removal of heavy metal ions. These shortcomings hinder their adsorption capacity from meeting the requirements. Therefore, it is necessary to modify natural zeolites to enhance their adsorption and ion exchange properties. Modification methods include acid treatment, alkaline treatment, heat treatment, ion exchange modification, microwave modification, organic modification, carrier modification, and framework modification.

Chitosan is a natural polymer that is nontoxic and a potential organic compound suitable for the removal of metal ions through chelation involving the amino and hydroxyl groups in the glucosamine units.[29] However, chitosan is soluble in acidic solutions and has poor mechanical stability, making it prone to aggregation and limiting its application range. Loading chitosan onto natural zeolite not only improves the mechanical stability of chitosan but also utilizes the porous structure and large specific surface area of zeolite. This adsorbent is environmentally friendly, safe, and nontoxic.

Therefore, this study successfully prepared a modified zeolite with chitosan loaded onto natural zeolite, which exhibited simplicity, a short reaction time, and high removal efficiency. In order to determine the optimal conditions for removing Cd(II) from low-concentration wastewater, various experimental parameters, including contact time, initial cadmium ion concentration, and pH value, were investigated. Additionally, adsorption isotherm models, adsorption kinetics, and thermodynamic studies were conducted. The morphological characteristics, X-ray diffraction (XRD), and Fourier transform infrared (FTIR) of the material were also determined. The results obtained serve as a foundation for the production and application of a novel adsorbent.

2. EXPERIMENTAL MATERIALS AND METHODS

2.1. Experimental Materials.

(1) The natural zeolite used in the experiment was procured from the Yusong Drainage Equipment Factory in Gongyi City, Henan Province, China. It belongs to the clinoptilolite group and is available in light gray, milky white, and flesh red colors. The particle size ranges from 0.5 to 1.5 mm. The primary physical and chemical analysis parameters for the zeolite are as follows: specific gravity, 2.16 g/cm^3; bulk density, 1.35 g/cm^3; abrasion rate, ≤0.8%; breakage rate, ≤1.0%; porosity, ≥50%; hydrochloric acid solubility, ≤2.26%; mud content, ≤1.0%; moisture content, ≤1.8%; ammonia adsorption capacity, 150−160 mmol/100 g; SiO_2 content, 68−71%; Al_2O_3 content, 13−14%; Fe_2O_3 content, 1−1.8%,; CaO content, 1.8−2.2%; MgO content, 0.9−1.4%; K_2O content, 1.6−3.9%; and Na_2O content, 0.6−1.6%.

(2) Chitosan: Food-grade chitosan with a degree of deacetylation of 95% was purchased from Zhengzhou Mingrui Chemical Products Co., Ltd.

2.2. Preparation Method of Chitosan-Loaded Natural Zeolite. *2.2.1. Pretreatment of Zeolite.*

(1) The natural zeolite was crushed using a grinder and then passed through a 40−60 mesh sieve to obtain natural zeolite particles with a particle size ranging from 0.3 to 0.45 mm.

(2) The crushed natural zeolite was rinsed with tap water until it became clear, followed by rinsing with distilled water to ensure cleanliness. Subsequently, the zeolite was soaked in deionized water for 24 h to dissolve impurities and reduce its acidity and alkalinity. Afterward, the zeolite was placed in a digital thermostatic drying oven at 105 °C for 24 h to dry. Once dried, it was cooled to room temperature, stored in sealed sample bags, and kept for further use.

2.2.2. Chitosan-Loaded Natural Zeolite Method. A certain concentration of chitosan solution was put into 100 mL beakers, and a certain amount of zeolite was slowly added to the mixture, which was stirred continuously for about 5 h at room temperature. After full infiltration, the mixture was left for 24 h, washed to neutrality with deionized water, and then placed in an electric thermostatic drying oven and dried to constant weight by a vacuum at 55 °C to obtain the chitosan-supported natural zeolite composite adsorption material.

2.3. Cr(VI) Adsorption Experiment. 8 g of chitosan-loaded natural zeolite (CNZ) was taken and placed in a conical flask. 100 mL of simulated wastewater was added containing an initial concentration of 100 μg/L of Cd(II). Under constant temperature at 25 °C and a stirring speed of 180 rpm, temperature-controlled shaking was performed for 180 min. After that, it was allowed to settle for 3 min, and the supernatant was collected from 1 cm below the liquid surface. The concentration of Cd(II) in the postadsorption wastewater using graphite furnace atomic absorption spectrophotometry on an atomic absorption spectrophotometer was measured.

The influence of CNZ dosage, initial pH value, temperature, adsorption time, initial concentration of cadmium ion solution, and other factors on the adsorption process was investigated by the single factor method. When investigating the effect of the dosage of chitosan-loaded natural zeolite (CNZ) on adsorption, the dosages of CNZ used were 0.2, 0.3, 0.4, 0.5, 0.6, 0.7, 0.8, and 0.9 g. When investigating the effect of the initial pH of the solution on adsorption, the initial pH values used were 2, 3, 4, 5, 6, 7, 8, 9, and 10. When investigating the effect of temperature on adsorption, the temperatures used were 25, 30, 45, and 65 °C. When investigating the effect of adsorption time at different temperatures (25, 45, and 65 °C), the adsorption times used were 10, 20, 30, 40, 60, 90, 120, 150, and 180 min. When investigating the effect of the initial concentration of cadmium ions on adsorption, the initial concentrations of cadmium ions used were 20, 40, 60, 80, and 100 μg/L.

2.4. Adsorption Efficiency. *2.4.1. Calculation of Removal Efficiency.* To calculate the removal efficiency of chitosan-loaded natural zeolite (CNZ) for cadmium, the removal rate is as follows

$$Y = \frac{100(C_0 - C_e)}{C_0} \quad (1)$$

https://doi.org/10.1021/acsomega.3c06041
ACS Omega 2024, 9, 573−584

where C_0 and C_e represent the initial concentration of Cd(II) (μg/L) and the concentration at which adsorption equilibrium is reached (μg/L), respectively.

2.4.2. Calculation of Cadmium Adsorption Capacity. The expression for the adsorption capacity of chitosan-loaded natural zeolite (CNZ) for cadmium is as follows

$$q_e = \frac{V(C_0 - C_e)}{m} \quad (2)$$

where q_e is the equilibrium adsorption capacity of adsorbent per unit mass (μg/g), C_0 is the initial concentration of cadmium (μg/L), and C_e is the equilibrium concentration of cadmium corresponding to q_e.

2.5. Adsorption Model. *2.5.1. Isothermal Adsorption Model.* The Langmuir and Freundlich equations were employed as isothermal adsorption models to investigate the adsorption behavior of zeolite toward Cd(II).

(1) Langmuir isothermal model: The Langmuir isothermal model assumes that a monolayer of molecules covers the surface of the adsorbent, and the adsorbate molecules on the solid surface experience identical forces and do not interact with each other. The expression for the model is

$$\frac{C_e}{q_e} = \frac{C_e}{q_m} + \frac{1}{q_m \cdot K_L} \quad (3)$$

where q_e is the monolayer adsorption capacity (μg/g); C_e is the equilibrium concentration of cadmium corresponding to q_e (μg/L); and q_m is the saturated adsorption capacity of monomolecular layer (μg/g); and K_L is the adsorption constant.

(2) Freundlich isothermal model

: The Freundlich isothermal model is based on multilayer adsorption on heterogeneous surfaces. The expression for the model is as follows

$$\ln q_e = \frac{1}{n}\ln C_e + \ln K_f \quad (4)$$

where q_e is the monolayer adsorption capacity (μg/g); C_e is the equilibrium concentration of cadmium corresponding to q_e (μg/L); K_f is the adsorption constant, n is the adsorption nonlinearity parameter, and n usually is greater than 1.

2.5.2. Thermodynamic Adsorption Model. Thermodynamic analysis of adsorption can evaluate the adsorption performance and the thermodynamic properties of the adsorption process. By considering thermodynamic parameters, such as the Gibbs free energy change (ΔG), entropy change (ΔS), and enthalpy change (ΔH), the thermal properties and spontaneity of the adsorption process can be determined.

The thermodynamic parameters can be calculated using the following formulas 5 and 6

$$\Delta G = -RT\ln K \quad (5)$$

$$\ln K = \frac{\Delta S}{R} - \frac{\Delta H}{RT} \quad (6)$$

where R is the gas constant with a value of 8.314 J/(mol·K); T is the absolute temperature in Kelvin (K); K is the equilibrium constant for the adsorption process; ΔG is the Gibbs free energy, kJ/mol; ΔH is the enthalpy change, kJ/mol; ΔS is the entropy change, J/(mol·K); and R is the ideal gas constant with a value of 8.3145 J/(mol·K).

According to eq 6, a linear regression analysis can be performed by plotting ln K against $1/T$. The slope and intercept of the fitted line can be used to calculate ΔH and ΔS, respectively. The spontaneity of the adsorption process can be determined by ΔG. If $\Delta G < 0$, the adsorption process is spontaneous; if $\Delta G > 0$, the adsorption process is non-spontaneous. The thermal nature of the adsorption process can be determined by ΔH. If $\Delta H < 0$, the adsorption process is exothermic; if $\Delta H > 0$, the adsorption process is endothermic. The disorder of the system during the adsorption process can be assessed by ΔS. If $\Delta S > 0$, the system's disorder and entropy increase, whereas if $\Delta S < 0$, the system becomes more ordered.

2.5.3. Adsorption Kinetic Model.

(1) Pseudo-first-order kinetic model: The pseudo-first-order kinetic equation describes the adsorption rate in terms of adsorption capacity and can explain the adsorption kinetics of various adsorbents. The differential equation expression for this model is as follows

$$\frac{dq_t}{dt} = k_1(q_e - q_t) \quad (7)$$

By integrating the above differential equation under boundary conditions (from $t = 0$ to $t = t$ and from $q_t = 0$ to $q_t = q_t$), a linear expression can be obtained

$$\lg(q_e - q_t) = \lg q_e - k_1 t \quad (8)$$

where q_t is the adsorption amount at time t, mg/g; t is the reaction time, min; k_1 is the rate constant of the adsorption reaction, min^{-1}; and q_e is the equilibrium adsorption capacity, mg/g.

(2) Pseudo-second-order kinetic model: The pseudo-second-order kinetic equation can be applied to the entire adsorption process. The differential equation expression for this model is as follows

$$\frac{dq_t}{dt} = k_2(q_e - q_t)^2 \quad (9)$$

By separating variables and integrating the above differential equation under boundary conditions (from $t = 0$ to $t = t$ and from $q_t = 0$ to $q_t = q_t$), a linear expression can be obtained

$$\frac{t}{q_t} = \frac{1}{k_2 q_e^2} + \frac{1}{q_e}t \quad (10)$$

where q_t is the adsorption amount at time t, mg/g; t is the reaction time, min; k_2 is the rate constant of the adsorption reaction, min^{-1}; and q_e is the equilibrium adsorption capacity, mg/g.

The intraparticle diffusion model, proposed by Weber and Morris, is based on the assumption that the adsorption rate is controlled by intraparticle diffusion. Its expression is as follows

$$q_t = K_{ip}t^{1/2} + C \quad (11)$$

where q_t is the adsorption amount at time t, mg/g; t is the reaction time, min; K_{ip} is the intraparticle diffusion constant, g/(min·min$^{1/2}$); and C is the boundary layer thickness, mg/g.

3. RESULTS AND DISCUSSION

3.1. Analysis of Factors Affecting Chitosan-Loaded Natural Zeolite. There are several factors that can influence the

https://doi.org/10.1021/acsomega.3c06041
ACS Omega 2024, 9, 573−584

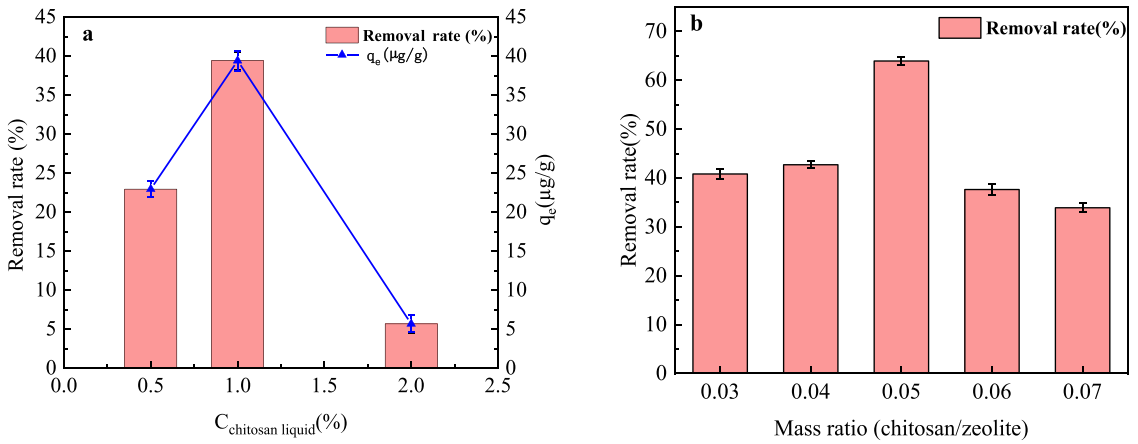

Figure 1. (a) Removal effect of natural zeolite loaded with chitosan of different concentrations on Cd(II). (b) Cd(II) removal effect of cadmium ions by the mass ratio of chitosan with natrual zeolite.

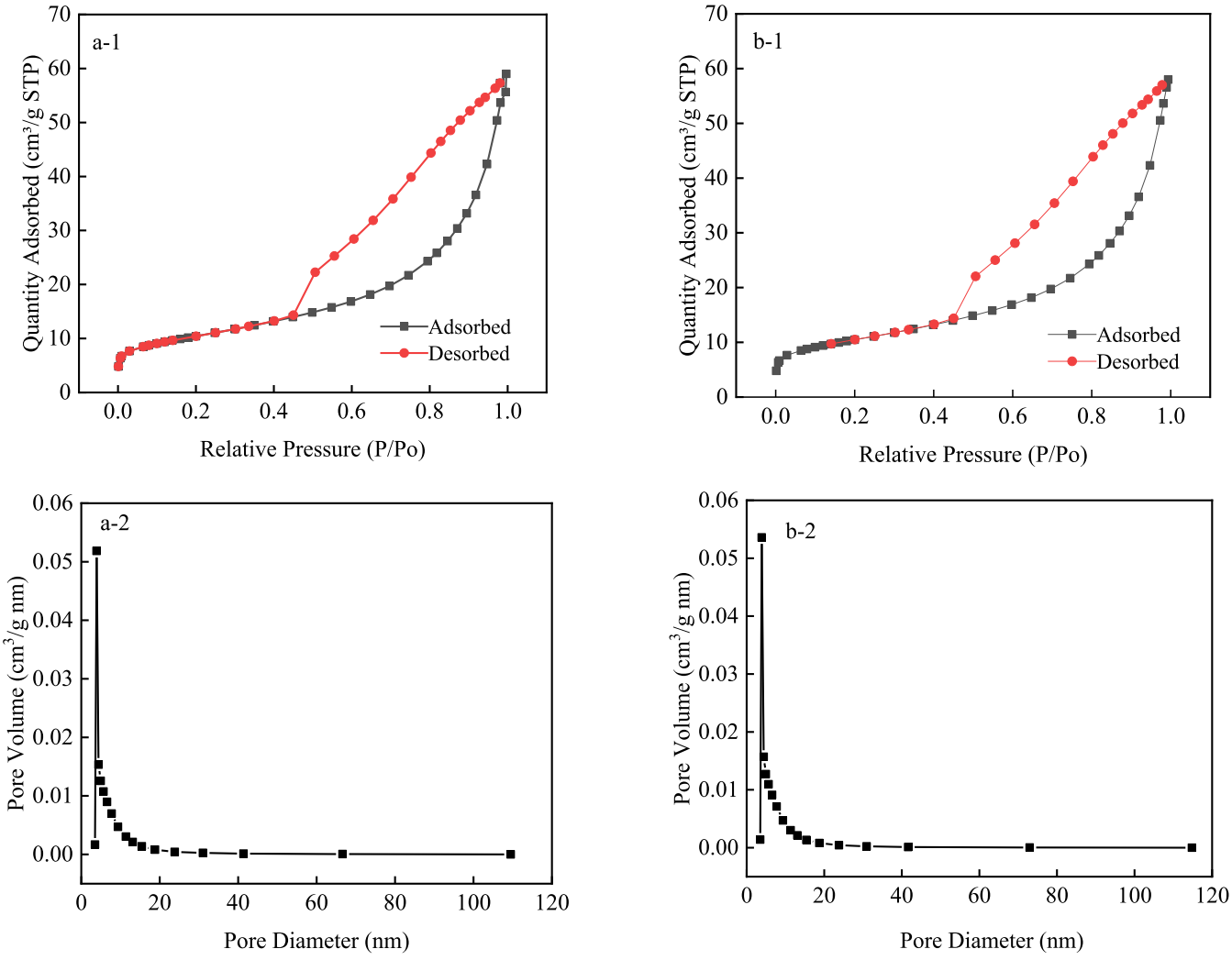

Figure 2. (a-1) Adsorption−desorption isotherm of natural zeolite, (a-2) pore size distribution of natural zeolite, (b-1) adsorption−desorption isotherm of chitosan-supported natural zeolite, and (b-2) pore size distribution of chitosan-supported natural zeolite.

loading of chitosan onto natural zeolite, including the type of zeolite, concentration of chitosan solution, mass ratio of chitosan to zeolite, modification time, and other aspects. In this experiment, the two most significant influencing factors, chitosan solution concentration and chitosan-to-zeolite mass ratio, were selected for the analysis of their effects on the modification process.

3.1.1. Influence of Chitosan Solution Concentration. Chitosan is insoluble in water but is soluble in an acetic acid solution. However, when the concentration of chitosan in acetic

https://doi.org/10.1021/acsomega.3c06041
ACS Omega 2024, 9, 573−584

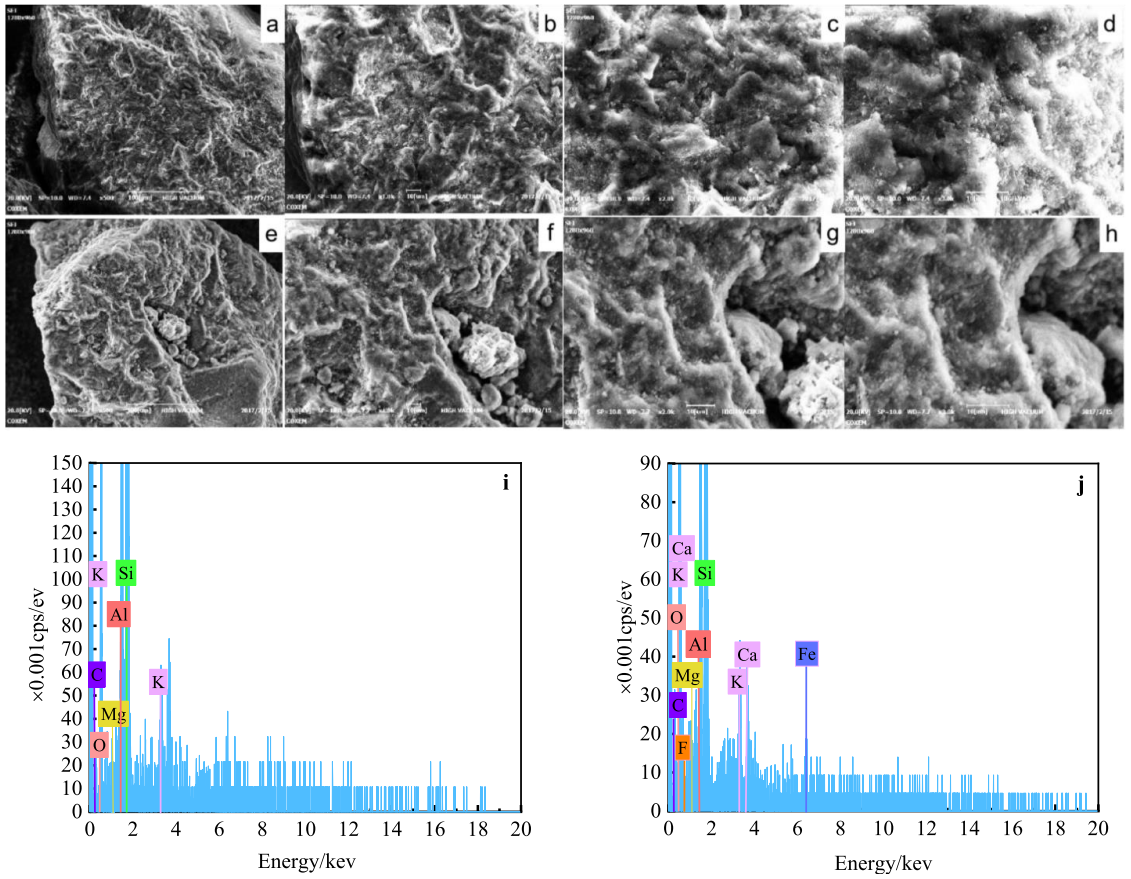

Figure 3. (a−d) SEM photograph of NZ and the SEM magnifications are 500, 1000, 2000, and 3000, respectively; (e−h) The SEM photograph of CNZ and the SEM magnifications are 500, 1000, 2000, and 3000, respectively; (i) EDS diagram of natural zeolite; (j) energy-dispersive spectrometry (EDS) of natural zeolite supported by chitosan.

acid solution exceeds 2%, the viscosity of the chitosan acetic acid solution increases, preventing sufficient contact with the zeolite.[30] Therefore, in this experiment, chitosan concentrations of 0.5, 1, and 2% were chosen.

The specific procedure involved placing 5 g of zeolite in each beaker with a mass ratio of 0.05 and adding an appropriate amount of chitosan solution at concentrations of 0.5, 1, and 2% (dissolved in 2% acetic acid). After stirring with a magnetic stirrer at room temperature for 1 h, the samples were rinsed with deionized water until neutral and then dried at 55 °C for subsequent use.

From Figure 1, conditions of chitosan-loaded natural zeolite with an additional amount of 0.1 g and a Cd(II) concentration of 100 μg/L in a simulated micropolluted water of 100 mL, the chitosan concentration of 1% yields the best adsorption effect for Cd(II), with a removal rate of 39.40%. At a chitosan concentration of 0.5%, the concentration is too low, resulting in a small amount of chitosan loaded on the zeolite, which does not effectively enhance the adsorption performance of the zeolite. At a chitosan concentration of 2.0%, the viscosity of the chitosan solution increases, hindering sufficient contact between chitosan molecules and zeolite, which, in turn, does not improve the adsorption performance of the zeolite. Therefore, for the preparation of chitosan-loaded natural zeolite, a chitosan solution concentration of 1.0% is chosen as the optimal condition.

3.1.2. Influence of Chitosan-to-Zeolite Mass Ratio. The mass ratio of chitosan/zeolite during the loading process affects the ratio of zeolite and chitosan in the resulting composite adsorbent. A too low chitosan loading ratio does not achieve the synergistic effect of chitosan and zeolite in adsorption, while an excessively high ratio leads to increased cost due to the high price of chitosan and ineffective utilization of zeolite. Therefore, the experiment was designed with chitosan-to-zeolite mass ratios of 0.03, 0.04, 0.05, 0.06, and 0.07.

The specific procedure involved taking chitosan and zeolite at the optimal zeolite loading concentration conditions and modifying the zeolite with chitosan at mass ratios of 0.03, 0.04, 0.05, 0.06, and 0.07.

From Figure 1, it can be observed that as the chitosan-to-natural zeolite mass ratio increases from 0.03 to 0.04, the removal rate of Cd(II) gradually improves for the chitosan/zeolite composite adsorbent. When the chitosan-to-natural zeolite mass ratio is 0.05, the modified zeolite shows the highest removal rate for Cd(II). This indicates that the composite adsorbent synergistically enhances the adsorption effect of Cd(II) through the combined adsorption of chitosan and zeolite. However, when the chitosan-to-natural zeolite mass ratio exceeds 0.05, there is a decreasing trend in the removal rate of Cd(II), suggesting that an excessively high mass ratio is unfavorable for improving the adsorption performance of the composite adsorbent. Therefore, the optimal preparation conditions for chitosan-loaded natural zeolite are a chitosan solution concentration of 1% and a chitosan-to-natural zeolite mass ratio of 0.05.

https://doi.org/10.1021/acsomega.3c06041
ACS Omega 2024, 9, 573−584

3.2. Chitosan-Loaded Natural Zeolite Characterization Analysis. *3.2.1. BET Surface Area and Pore Size Analysis.* The nitrogen adsorption−desorption isotherms and corresponding structural characteristics of natural zeolite and chitosan-loaded natural zeolite are shown in Figure 2. According to the classification by the International Union of Pure and Applied Chemistry, both the nitrogen adsorption−desorption isotherms of natural zeolite and chitosan-loaded natural zeolite belong to type IV adsorption isotherms.[31] The hysteresis loop formed between the adsorption and desorption isotherms belongs to the H3 type,[32] indicating that the materials have mesoporous layered structures with narrow slit-like pores, as well as the presence of voids and micropores.[33]

According to the nitrogen adsorption−desorption isotherm analysis, the specific surface area of chitosan-loaded natural zeolite is determined to be 30.65 m^2/g, with a pore volume of 0.068 cm^3/g. The average pore size of natural zeolite is determined to be 9.80 nm, while the average pore size of chitosan-loaded natural zeolite is 9.50 nm, which is consistent with previous studies.[34] The BET surface area of chitosan-loaded natural zeolite (CNZ) increases compared to the natural zeolite, while the total pore volume remains relatively unchanged and the average pore size slightly decreases. This could be attributed to the thorough contact between natural zeolite and chitosan solution during 5 h of stirring, followed by soaking for 24 h. Some chitosan molecules may enter the large pore channels of natural zeolite, while others may cover the surface of natural zeolite, leading to a slight decrease in the average pore size of natural zeolite.

3.2.2. Scanning Electron Microscopy (SEM/EDS) Analysis. Figure 3a−h shows the scanning electron microscopy (SEM) images of natural zeolite (NZ) and chitosan-loaded natural zeolite (CNZ). The SEM images were taken at magnifications of 500, 1000, 2000, and 3000. Additionally, the chemical composition of natural zeolite and chitosan-loaded natural zeolite was analyzed by energy-dispersive spectroscopy (EDS), as shown in Figure 3i,j, and Table 1.

Table 1. Element Distribution of the Various Adsorbents Determined by Energy-Dispersive X-ray Detector

	element content (wt %)				
name of the material	O	Si	C	Al	K
NZ	35.10	27.87	12.27	10.19	1.21
CNZ	39.89	26.77	13.23	8.89	2.49

From Figure 3a−d, it can be observed that natural zeolite (NZ) has a smooth and irregular plate-like surface structure with some pores. The internal structure is relatively uniform and dense. In Figure 3e−h, it is clearly visible that chitosan-loaded natural zeolite (CNZ) has finer powdery particles adhering to the surface and some thick plate-like pores, which correspond to the chitosan particles. This indicates that chitosan has been successfully loaded onto the surface and partial pores of natural zeolite.

From Figure 3i,j, the main elements of natural zeolite are O, Si, C, and Al, with a small amount of K. In combination with the observed plate-like structure in the scanning electron microscope, this confirms the porous aluminosilicate nature of natural zeolite. The main elements of chitosan-loaded natural zeolite are O, Si, C, and Al. After modification with chitosan, the content of O in the chitosan-loaded natural zeolite increased from 35.10 to 39.89%, and the content of C increased from 12.27 to 13.23%. This is because chitosan contains O and C elements, indicating that chitosan has been successfully loaded onto the natural zeolite.

3.2.3. XRD Analysis. X-ray diffraction spectroscopy was performed to characterize the natural zeolite (NZ) and chitosan-loaded natural zeolite (CNZ) adsorbents, and the results are shown in Figure 4a.

From Figure 4a, it can be observed that natural zeolite (NZ) exhibits relatively strong diffraction peaks at X-ray diffraction angles (2θ) of 9.81, 11.18, 13.04, 13.80, 16.88, 17.33, 22.28, 22.42, 26.67, and 30.24°. Compared with the X-ray diffraction spectra of natural zeolite (NZ) and chitosan-loaded natural zeolite (CNZ), it is found that the positions and number of diffraction peaks remain unchanged and the X-ray diffraction spectra of both materials exhibit similar shapes. This indicates that chitosan-loaded natural zeolite undergoes physical mixing rather than chemical changes, and the crystal structure of chitosan-loaded natural zeolite (CNZ) remains unchanged. In the X-ray diffraction spectrum of chitosan-loaded natural zeolite (CNZ), a unique diffraction peak appears at an X-ray diffraction angle of 2θ = 26.87°, which corresponds to the chitosan diffraction peak reported in the literature,[35] indicating that chitosan has been successfully loaded onto the natural zeolite.

3.2.4. Fourier Infrared spectroscopy (FTIR) Analysis. The infrared spectra of natural zeolite (NZ) and chitosan-loaded natural zeolite (CNZ) were determined using Fourier-transform infrared spectroscopy, and the spectra are shown in Figure 4b.

From Figure 4b, it can be observed that natural zeolite exhibits absorption peaks in the range of 3000−3630 cm^{-1}, corresponding to stretching vibrations of −OH groups. The absorption peak at 1650 cm^{-1} is primarily due to the bending vibrations of adsorbed water molecules, while the peak at 1075 cm^{-1} results from the asymmetric stretching vibrations of Al−O tetrahedra. The absorption peaks at 700 and 490 cm^{-1} are mainly attributed to symmetric stretching and bending vibrations of Si−O and Al−O bonds, respectively. Chitosan-loaded natural zeolite, on the other hand, shows overlapping absorption peaks in the range of 3000−3630 cm^{-1}, corresponding to stretching vibrations of −OH and $-NH_2$ groups. The absorption peak at 1075 cm^{-1} is still associated with the asymmetric stretching vibrations of the Al−O tetrahedra. The absorption peaks at 700 and 490 cm^{-1} continue to be primarily attributed to symmetric stretching and bending vibrations of Si−O and Al−O bonds, respectively.

The positions of the infrared spectroscopy characteristic peaks of natural zeolite (NZ) did not undergo significant changes before and after modification. This indicates that the basic structure of natural zeolite remains unaffected after loading with chitosan and that chitosan-loaded natural zeolite (CNZ) still retains the framework structure of zeolite tetrahedra. The intensities of peaks at different positions have varied to different extents, with an increase in the peak area observed for CNZ. Additionally, in conjunction with the literature (Tan, 2018), it is evident that chitosan-loaded natural zeolite exhibits vibrational bands at 1586 and 3550 cm^{-1}, corresponding to $-NH_2$ and −OH functional groups, which are typical active groups in the chitosan molecular structure. This phenomenon provides confirmation that chitosan has indeed been successfully loaded onto the framework of the natural zeolite.

3.3. Analysis of Influencing Factors of Adsorption. *3.3.1. Influence of Chitosan Supported Natural Zeolite (CNZ) Dosage on Cadmium Ion Adsorption Effect.* The effect of the chitosan-loaded natural zeolite (CNZ) dosage on the adsorption of cadmium ions in water is shown in Figure 5a. From Figure 5a,

https://doi.org/10.1021/acsomega.3c06041
ACS Omega 2024, 9, 573−584

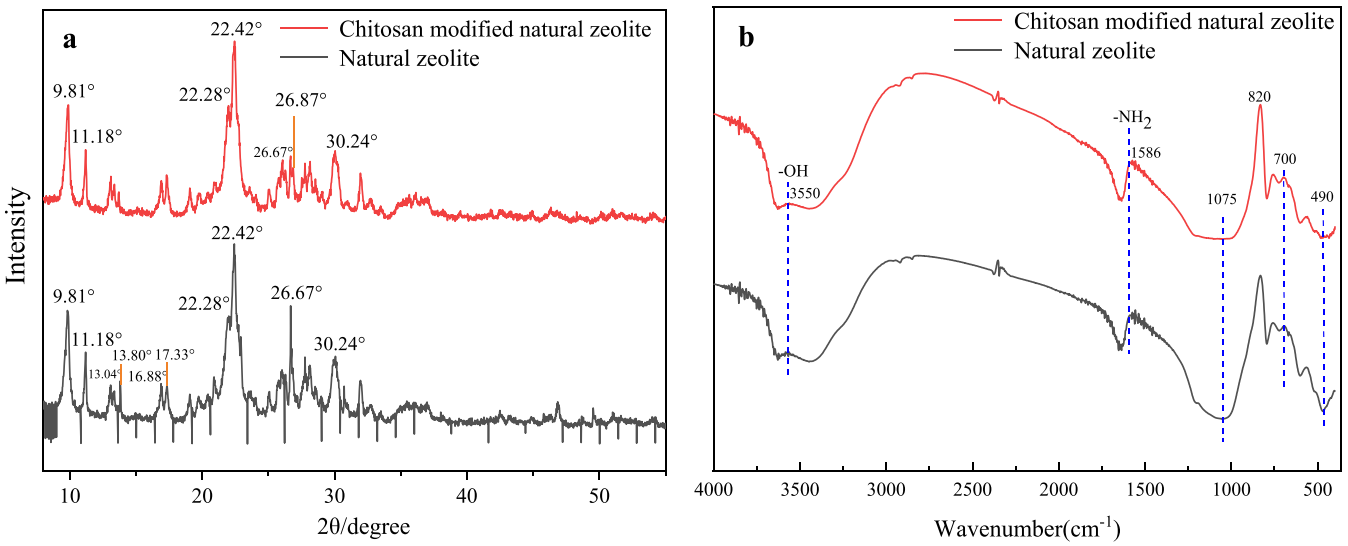

Figure 4. (a) XRD power pattern of NZ and modified zeolite. (b) FTIR spectrometer of NZ and modified zeolite.

it can be observed that as the dosage increases, the adsorption capacity gradually decreases, while the removal efficiency of cadmium ions by chitosan-loaded natural zeolite (CNZ) increases and then stabilizes. When the dosage is 8 g/L, the removal efficiency of Cd(II) by chitosan-loaded natural zeolite (CNZ) reaches 91.35%, with an adsorption capacity of 114.2 μg/L. When the dosage is 9 g/L, the removal efficiency of cadmium(II) by chitosan-loaded natural zeolite (CNZ) reaches 91.52%, with a similar removal effect.

3.3.2. Effect of Initial pH Value of Solution on Adsorption of Cadmium Ions. The influence of the initial pH value of the solution on the removal efficiency of cadmium ions is shown in Figure 5b. From Figure 5b, it can be observed that within the pH range of 2−4, the removal efficiency of cadmium ions in water by the composite adsorbent chitosan-loaded natural zeolite (CNZ) increases rapidly with an increasing pH value. However, when the pH value is 6, the removal efficiency of cadmium ions by chitosan-loaded natural zeolite (CNZ) reaches the highest value at 92.06%, and the adsorption capacity of Cd(II) also reaches its maximum at 115.1 μg/g. When the pH is between 7 and 9, the removal efficiency of natural zeolite loaded with chitosan (CNZ) composite adsorbent for cadmium ions in water decreases with an increase in pH. When the pH value is above 9, both the removal efficiency and the adsorption capacity of Cd(II) increase.

3.3.3. Effect of Temperature on Adsorption of Cadmium Ions. The influence of the adsorption temperature on the removal efficiency of cadmium ions is shown in Figure 5c. From Figure 5c, it can be observed that as the temperature increases, the removal efficiency of cadmium(II) by the composite adsorbent chitosan-loaded natural zeolite (CNZ) gradually increases, but the increase is not significant. At different temperatures, the removal efficiency remains above 90%. At a temperature of 25 °C, the removal efficiency of cadmium(II) by chitosan-loaded natural zeolite (CNZ) reaches 93.44%, indicating a significant adsorption capacity of chitosan-loaded natural zeolite (CNZ) for low concentrations of Cd(II), and the adsorption process can be inferred as an endothermic reaction. In practical applications, increasing the temperature will increase operational costs and may not be economically viable. Therefore, considering the economic perspective, for subsequent experiments on other influencing factors, the adsorption time can be set at 25 °C for 90 min to ensure sufficient time for the reaction to reach adsorption equilibrium.

3.3.4. Influence of Initial Concentration of Cadmium Ions on Adsorption Effect. The effect of the initial concentration of cadmium ions on the removal of Cd(II) by the composite adsorbent, chitosan-loaded natural zeolite (CNZ), is shown in Figure 5e. From Figure 5e, it can be observed that as the initial concentration of cadmium ion solution increases, the adsorption removal rate of Cd(II) by CNZ gradually decreases along with a gradual decrease in adsorption capacity. The main reason for this is that the amount of chitosan-loaded natural zeolite (CNZ) used is constant, and the adsorption capacity is limited. When the solution concentration increases, the adsorption amount increases, leading to a decrease in the adsorption rate of Cd(II) by the composite adsorbent CNZ. When the initial concentration of the solution is above 40 μg/L, there is a significant change in the adsorption of Cd(II) by CNZ. Therefore, the most suitable concentration of the solution containing cadmium ions is 40 μg/L, where the composite adsorbent CNZ achieves the highest removal rate of Cd(II), reaching 97.82%.

3.4. Analysis of Adsorption Mechanism. *3.4.1. Adsorption Isotherm Analysis of Ccadmium Ions by Chitosan-Supported Natural Zeolite (CNZ).* The Langmuir adsorption isotherms at 25, 45, and 65 °C are shown in Figure 6a. The values of Q_m and K can be calculated from the slopes and intercepts of the obtained lines.

The Freundlich adsorption isotherms at 25, 45, and 65 °C are shown in Figure 6b. The values of K and n can be calculated from the slopes and intercepts of the obtained lines.

The parameters of the adsorption isotherm models obtained from Figure 6a,b, as well as the specific parameter data, are shown in Table 2.

From Figure 6a,b, and Table 2, it can be observed that at three temperatures of 25, 45, and 65 °C, the correlation coefficients for the Langmuir adsorption isotherm model are 0.9997, 0.9999, and 0.9997, all greater than 0.999. On the other hand, the correlation coefficients for the Freundlich adsorption isotherm model are 0.8253, 0.3678, and 0.9264, indicating a relatively poor fit. This suggests that the Langmuir adsorption isotherm model is applicable to the adsorption process of chitosan-loaded natural zeolite (CNZ) at low-concentration Cd(II) in water, which is consistent with the findings in the literature,[36] regarding

https://doi.org/10.1021/acsomega.3c06041
ACS Omega 2024, 9, 573−584

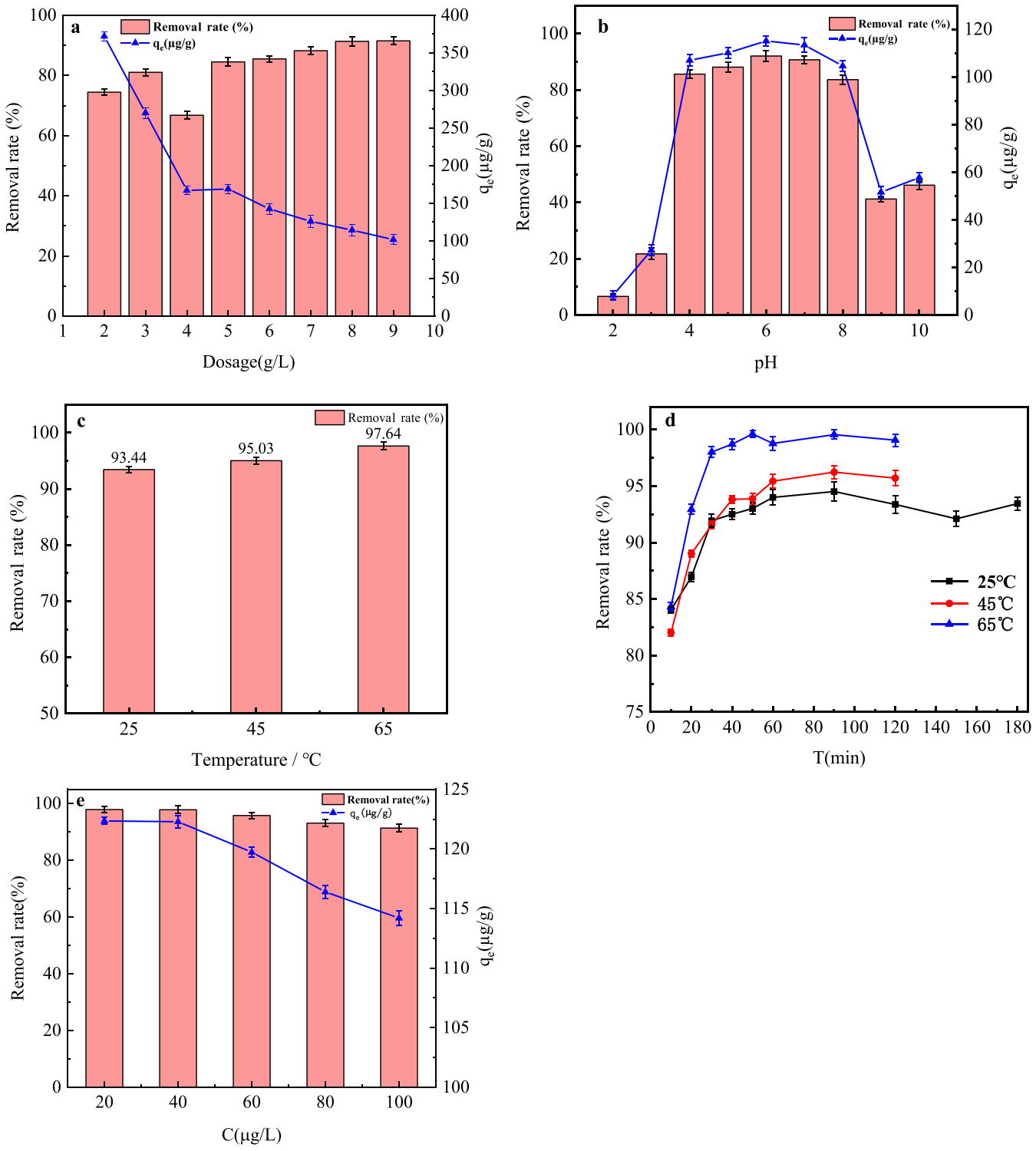

Figure 5. (a) Effect of CNZ dosage on Cd(II) removal; (b) effects of solution pH on Cd(II) removal by CNZ; (c) effects of temperature on Cd(II) removal by CNZ; (d) effects of reaction time on Cd(II) removal by CNZ at different temperatures; and (e) effects of initial concentration on Cd(II) removal by CNZ.

the adsorption process of chitosan-loaded natural zeolite (CNZ). It also implies that the adsorption process of chitosan-loaded natural zeolite (CNZ) follows a monolayer adsorption mechanism. By fitting the Langmuir isotherm equation, we can also determine the theoretical maximum adsorption capacity of chitosan-loaded natural zeolite (CNZ) for Cd(II) at different temperatures of 25, 45, and 65 °C, which are 112.4, 123.5, and 116.3 μg/g, respectively.

3.4.2. Thermodynamic Analysis of Cadmium Ion Adsorption by Chitosan-Loaded Natural Zeolite (CNZ). The adsorption efficiency of the adsorbent for Cd(II) at different temperatures provides a visual representation of the temperature's impact on the adsorption process. To calculate the thermodynamic parameters of adsorption, the natural logarithm of the equilibrium constant ($\ln K_c$) is plotted against the reciprocal of temperature ($1/T$), as shown in Figure 6c. From

https://doi.org/10.1021/acsomega.3c06041
ACS Omega 2024, 9, 573−584

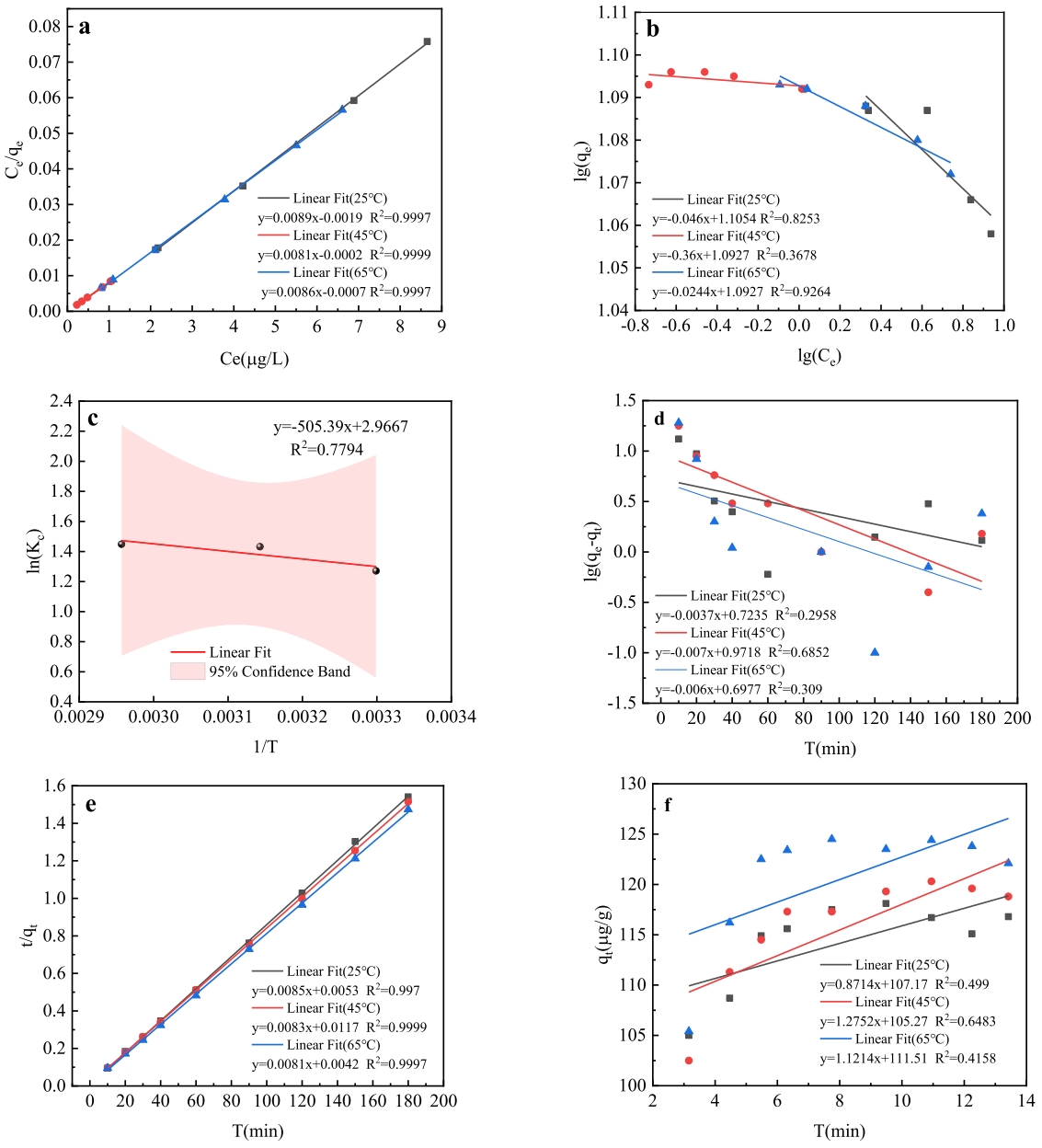

Figure 6. (a) Langmuir adsorption isotherms of natural zeolite (CNZ) supported by chitosan at 25, 45, and 65 °C, respectively; (b) Freundlich adsorption isotherms for chitosan-supported natural zeolite (CNZ) at 25, 45, and 65 °C, respectively; (c) thermodynamical model of CNZ; (d) pseudo-first-order kinetic equation of the adsorption rate of Cd(II) by chitosan-supported natural zeolite (CNZ) at 25, 45, and 65 °C, respectively; (e) pseudo-second-order kinetic equation of the adsorption rate of Cd(II) by chitosan-supported natural zeolite (CNZ) at 25, 45, and 65 °C, respectively; and (f) intraparticle diffusion kinetics of the adsorption from Cd(II) by CNZ at 25, 45, and 65 °C, respectively.

Table 2. Adsorption Isotherm Constant of the Langmuir and Freundlich of CNZ

	Langmuir model			Freundlich model		
temperature (°C)	K (g/μg)	Q_m (μg/g)	R^2	lgk	1/n	R^2
25	4.6	112.4	0.9997	1.1054	0.0460	0.8253
45	405.0	123.5	0.9999	1.0927	0.0036	0.3678
65	12.3	116.3	0.9997	1.0927	0.0244	0.9264

Table 3. Values of Thermodynamic Parameters for the Adsorption of Cd(II) Ions on CNZ

T (K)	ΔG (kJ/mol)	ΔH (kJ/mol)	ΔS (J/mol·K)
303.15	3.202	4.202	24.67
318.15	3.608		
338.15	3.830		

the resulting straight line in Figure 6c, the slope and intercept of the line can be used to calculate the values of ΔH, ΔS, and ΔG, as shown in Table 3.

From Table 3, it can be observed that at 25, 45, and 65 °C, the calculated values of Gibbs free energy (ΔG) are −3202.347, −3607.650, and −3830.334 kJ/mol, respectively. All values are negative, indicating that the adsorption process of Cd(II) by chitosan-loaded natural zeolite (CNZ) is spontaneous. The enthalpy value (ΔH) is 4202.07 kJ/mol, which is positive, suggesting an endothermic reaction in the adsorption process of Cd(II) by chitosan-loaded natural zeolite (CNZ). The entropy

https://doi.org/10.1021/acsomega.3c06041
ACS Omega 2024, 9, 573−584

Table 4. Comparison of Kinetic Model Rate Constants

		quasi-first-order kinetic equation			pseudo-second-order kinetic equation			internal diffusion dynamics equation		
T (°C)	q_e	K_1	q_1	R^2	K_2	q_2	R^2	K_3	C	R^2
25	118.1	0.009	5.29	0.2958	0.014	117.65	0.9997	0.8714	107.17	0.499
45	120.3	0.016	9.37	0.6852	0.006	120.5	0.9999	1.2752	105.27	0.6483
65	124.5	0.014	4.99	0.3090	0.016	123.5	0.9997	1.1214	111.51	0.4158

value (ΔS) is 24.67 J/mol·K, which is positive, indicating an increase in entropy during the adsorption process of Cd(II) by chitosan-loaded natural zeolite (CNZ). These results are consistent with the findings in the literature (Li, 2020), regarding the entropy increase during the adsorption process.

3.4.3. Kinetic Analysis of Cadmium Ion Adsorption by Chitosan-Loaded Natural Zeolite (CNZ). The adsorption removal rate of the adsorbent for Cd(II) at different temperatures provides a visual representation of the temperature's impact on the adsorption process. To calculate the kinetic parameters of adsorption, the natural logarithm ($q_e - q_t$) is plotted against temperature (T), as shown in Figure 6d–f. From the resulting straight line in Figure 6d–f, the slope and intercept of the line can be used to calculate the values of K, q, and R^2, as shown in Table 4.

By using the pseudo-first-order kinetic equation and calculating the experimental data, a pseudo-first-order kinetic equation for the adsorption rate of Cd(II) by chitosan-loaded natural zeolite (CNZ) at 25, 45, and 65 °C is obtained, as shown in Figure 6d.

Similarly, by using the pseudo-second-order kinetic equation and calculating the experimental data, a pseudo-second-order kinetic equation for the adsorption rate of Cd(II) by chitosan-loaded natural zeolite (CNZ) at 25, 45, and 65 °C is obtained, as shown in Figure 6e.

Furthermore, by using the intraparticle diffusion kinetics in eq 11 and calculating the experimental data, a linear fit of q_t against $t^{1/2}$ is obtained, representing the intraparticle diffusion kinetic equation for the adsorption rate of Cd(II) by chitosan-loaded natural zeolite (CNZ) at 25, 45, and 65 °C, as shown in Figure 6f.

Figures 6d,e and S6f represent the linear fits of the first-order, second-order, and intraparticle diffusion equations, respectively, at 25, 45, and 65 °C. By calculating the slope and intercept of these linear equations, the adsorption rate constants, equilibrium adsorption capacities, and the coefficient of determination (R^2) for each kinetic equation can be obtained, as shown in Table 4.

From the linear fitting and correlation coefficients obtained from Figure 6d,e, it can be observed that the pseudo-second-order kinetic equation provides the best fit for the adsorption data of Cd(II) onto chitosan-loaded natural zeolite (CNZ). Furthermore, based on the experimental data, it is found that the equilibrium adsorption time of Cd(II) on CNZ is 60 min at temperatures of 25, 45, and 65 °C, with the corresponding equilibrium adsorption capacities of 118.1, 120.3, and 124.5 μg/g, respectively. Referring to the adsorption kinetic parameters in Table 4, the theoretical equilibrium adsorption capacities (q_e) at temperatures of 25, 45, and 65 °C are calculated to be 117.65, 120.5, and 123.5 μg/g, respectively, using the pseudo-second-order kinetic model. The calculated theoretical equilibrium adsorption capacities are closer to the experimental equilibrium adsorption capacities. This finding is consistent with the adsorption kinetics process described in ref 34. Therefore, it can be concluded that the pseudo-second-order adsorption kinetic mechanism predominantly governs the adsorption of Cd(II) onto chitosan-loaded natural zeolite (CNZ) during the adsorption process.

From the linear fitting of the intraparticle diffusion model in Figure 6f, it can be observed that the line does not pass through the origin. Therefore, it can be inferred that intraparticle diffusion is not the sole rate-controlling step in the adsorption process of a Cd(II) solution onto chitosan-loaded natural zeolite (CNZ). Overall, the adsorption process of the Cd(II) solution onto CNZ is likely controlled by a combination of surface adsorption on chitosan-loaded natural zeolite (CNZ) active sites and intraparticle diffusion adsorption.

4. CONCLUSIONS

(1) Chitosan-loaded natural zeolite (CNZ) was successfully prepared through the experiment. The optimal modification conditions for chitosan-loaded natural zeolite were a concentration of 1% chitosan solution (dissolved in 2% acetic acid) and a chitosan-to-zeolite mass ratio of 0.005.

(2) The structure and performance of CNZ were improved after modification. The specific surface area of CNZ increased, and the surface morphology became more porous, with finer powdery particles adhering to the surface. Both oxygen (O) and carbon (C) elements showed a significant increase, while the crystal structure remained unchanged. Additionally, the infrared spectrum of CNZ exhibited vibration bands corresponding to $-NH_2$ and −OH, indicating the successful loading of chitosan onto the zeolite filter material.

(3) The optimal conditions for chitosan-loaded natural zeolite as an adsorbent to remove Cd(II) were as follows: a temperature of 25 °C, a pH of 6, a dosage of 8 g/L, and an adsorption reaction time of 60 min. Under these conditions, the removal efficiency of chitosan-loaded natural zeolite (CNZ) for a 100 μg/L cadmium solution in a volume of 100 mL reached above 94.51%.

(4) The adsorption of Cd(II) on chitosan-loaded natural zeolite (CNZ) followed the Langmuir adsorption isotherm model, indicating monolayer adsorption. At a temperature of 25 °C, the maximum theoretical adsorption capacity of Cd(II) was 112.4 μg/g. The adsorption process followed pseudo-second-order kinetics. Thermodynamically, the adsorption process was spontaneous and endothermic, with an increase in entropy during the adsorption process.

■ ASSOCIATED CONTENT

Data Availability Statement

The data sets generated and/or analyzed during the current study are available upon request by contact with the corresponding author.

https://doi.org/10.1021/acsomega.3c06041
ACS Omega 2024, 9, 573−584

Supporting Information

The Supporting Information is available free of charge at https://pubs.acs.org/doi/10.1021/acsomega.3c06041.

Research purpose, research methods, and research results of this proposal, along with the references; recent relevant papers; differences between this proposal and recent relevant papers; separate answers to the three questions: Why this Topic? Why these Authors? Why Now? (PDF)

AUTHOR INFORMATION

Corresponding Author

Yan Shi − *School of Environmental and Municipal Engineering, North China University of Water Resources and Electric Power, Zhengzhou 450046, China; Collaborative Innovation Center for Effifficient Utilization of Water Resources, Zhengzhou 450046, China;* orcid.org/0000-0002-3083-1361; Email: syshiyan2022@126.com

Authors

Xin Wang − *School of Environmental and Municipal Engineering, North China University of Water Resources and Electric Power, Zhengzhou 450046, China*

Changping Feng − *School of Environmental and Municipal Engineering, North China University of Water Resources and Electric Power, Zhengzhou 450046, China*

Weiwei Chen − *School of Environmental and Municipal Engineering, North China University of Water Resources and Electric Power, Zhengzhou 450046, China*

Shipeng Yang − *School of Environmental and Municipal Engineering, North China University of Water Resources and Electric Power, Zhengzhou 450046, China*

Complete contact information is available at: https://pubs.acs.org/10.1021/acsomega.3c06041

Author Contributions

Y.S. designed the research; X.W. and C.F. performed specific experiments, W.C. and S.Y. analyzed the data, and Y.S. and X.W. wrote and revised the paper.

Notes

The authors declare no competing financial interest.

Ethical Approval This manuscript does not involve ethical approval.

Consent to Publish All authors have read and agreed to the published version of the manuscript.

ACKNOWLEDGMENTS

The research was partially supported by Training Plan for Young Backbone Teachers in Colleges and Universities in Henan Province (2019GGJS098 and 2020GGJS098) and Master Innovation Ability Improvement Project of North China University of Water Resources and Electric Power.

REFERENCES

(1) Ren, J.; Liu, X.; Wu, Y.; Zhang, J.; Cao, T.; Li, J.; et al. The evaluation and content of typical contaminants in irrigation water during the slackseason in the suburban areas of North River and West River Delta. *Acta Sci. Circumstantiae* **2020**, *40* (11), 3990−4000.

(2) Meng, W.; Wang, Z.; Hu, B.; Wang, Z.; Li, H.; Goodman, R. C. Heavy metals in soil and plants after long-term sewage irrigation at Tianjin China: A case study assessment. *Agric. Water Manage.* **2016**, *171*, 153−161.

(3) Zhao, F.; Ma, Y.; Zhu, Y. G.; Tang, Z.; McGrath, S. Soil contamination in China: current status and mitigation strategies. *Environ. Sci. Technol.* **2015**, *49* (2), 750−759.

(4) Guo, W.; Du, Y.; Liang, C.; Wu, Y.; Lin, D.; Zhang, X.; et al. Effects of Natural and Ammonium Chloride/Calcium Chloride-Modified. *Chin. J. Soil Sci.* **2019**, *50* (3), 719−724.

(5) Shao, J.; Liu, C.; Yan, X.; Yang, L.Cadmium distribution characteristics and environmental risk assessment in typical sewage irrigation area of Hebei Province *Acta Sci. Circumstantiae* 2019; Vol. *39* 3, pp 917−927.

(6) Zhong-ying, N. I.; Guo-xiong, X. I.; Zhang, M. K. Research Progress on Remediation Technology of Cadmium-contaminated Agricultural Soils. *Anhui Agric. Sci. Bull.* **2017**, *23* (6), 115−120.

(7) Zhu, P.; Liang, X.; Wang, P.; Wang, J.; Gao, Y.; Hu, A.; et al. Assessment of dietary cadmium exposure: a cross-sectional study in rural areas of south China. *Food Control* **2016**, *62*, 284−290.

(8) Quadros, I. P. S.; Madeira, N. N.; Loriato, V. A. P.; Saia, T. F. F.; Silva, J. C.; Soares, F. A. F.; et al. Cadmium-mediated toxicity in plant cells is associated with the DCD/NRP-mediated cell death response. *Plant Cell Environ.* **2022**, *45* (2), 556−571.

(9) Abu-Shahba, M. S.; Mansour, M. M.; Mohamed, H. I.; Sofy, M. R. Effect of biosorptive removal of cadmium ions from hydroponic solution containing indigenous garlic peel and mercerized garlic peel on lettuce productivity. *Sci. Hortic.* **2022**, *293*, No. 110727, DOI: 10.1016/j.scienta.2021.110727.

(10) Huang, D.; Zhu, Q.; Zhu, H.; Xu, C.; Liu, S. Advances and prospects of safety agro-utilization of heavy metal contaminated farmland soil. *Res. Agric. Modernization* **2018**, *39* (6), 1030−1043.

(11) Zheng, J.; Li, Y.; Xu, D.; Zhao, R.; Liu, Y.; Li, G.; et al. Facile fabrication of a positively charged nanofiltration membrane for heavy metal and dye removal. *Sep. Purif. Technol.* **2022**, *282*, No. 120155.

(12) Abdel-Hakim, A.; Abdella, A. H.; Sabaa, M. W.; Gohar, H. Y.; Mohamed, R. R.; Tera, F. M. Performance evaluation of modified fabricated cotton membrane for oil/water separation and heavy metal ions removal. *J. Vinyl Addit. Technol.* **2021**, *27* (4), 933−945, DOI: 10.1002/vnl.21866.

(13) Wu, B.; Weng, X. D.; Wang, N.; Yin, M. J.; Zhang, L.; An, Q. F. Chlorine-resistant positively charged polyamide nanofiltration membranes for heavy metal ions removal. *Sep. Purif. Technol.* **2021**, *275*, No. 119264.

(14) Sreeramareddygari, M.; Shivanna, J. M.; Somasundrum, M.; Soontarapa, K.; Surareungchai, W. Polythiocyanuric acid-functionalized MoS_2 nanosheet-based high flux membranes for removal of toxic heavy metal ions and congo red. *Chem. Eng. J.* **2021**, *425*, No. 130592, DOI: 10.1016/j.cej.2021.130592.

(15) Giri, A. K.; Cordeiro, M. Heavy Metal Ion Separation from Industrial Wastewater using Stacked Graphene Membranes: A Molecular Dynamics Simulation Study. *J. Mol. Liq.* **2021**, *338* (5), No. 116688.

(16) Hussain, S. T.; Ali, S. A. Removal of Heavy Metal by Ion Exchange Using Bentonite Clay. *J. Ecol. Eng.* **2021**, *22* (1), 104−111.

(17) Zhao, X.; Cheng, Q.; Wang, W.; Ning, X.; Cheng, W.; Cao, H.; Kang, M.; Wang, Y.Study on Vanadium Extraction from Leachate of Low Grade Vanadium Ore by Ion Exchange Method *Conserv. Util. Miner. Resour.* 2022; Vol. *42* 03, pp 69−74.

(18) Shi, Y.; Wang, X.; Feng, C.; et al. Technologies for the Removal of Antibiotics in the Environment: a Review. *Int. J. Electrochem. Sci.* **2022**, *17*, No. 220768, DOI: 10.20964/2022.07.74.

(19) Hunsom, M.; Pruksathorn, K.; Damronglerd, S.; et al. Electrochemical treatment of heavy metals (Cu~(2+), Cr~(6+), Ni~(2+)) from industrial effluent and modeling of copper reduction. *Water Res.* **2005**, *39* (4), 610−616.

(20) Olshanskaya, L. N.; Valiev, R. S.; Osipova, T. V. A merthod for accelerting electrochemical phytoremediation of waste water from heavy metal ions when exposed to phytosorbend plants by physical fields. *Environ. Sci.* **2020**, *1* (29), 132−143, DOI: 10.35264/1996-2274-2020-1-132-143.

(21) Saloua, J.; Mohamed, T.; Ahmed, M.; Khadija, M. Industrial rejection: removal of heavy metals based on chemical precitation and

research for recoverable material in byproducts. *Int. J. Eng. Technol. Manage. Res.* **2020**, *7* (2), 39−52.
(22) Zhang, G.; Zhang, D. Experimental Study on the Treatment of Heavy Metal in Electroplating Wastewater by Chemical Precipitation Method *Shandong Chem. Ind.* 2016.
(23) Li, D. W.; Yuan, X.; Wang, K.; Yang, J.; Li, D.Experiment of the Wastewater Treatment with the Method of Secondary Chemical Precipitation Ferrite *J. Chongqing Jianzhu Univ.* 2007; Vol. *11* 2, pp 17−25.
(24) Li, Z.; Wang, L.; Meng, J.; Liu, X.; Xu, J.; Wang, F.; et al. Zeolite-supported nanoscale zero-valent iron: New findings on simultaneous adsorption of Cd(II), Pb(II), and As(III) in aqueous solution and soil. *J. Hazard. Mater.* **2018**, *344*, 1−11.
(25) Yang, Q.; Chen, C.; Zhao, C.; Sun, M.; Chen, Z.Removal of heavy metalion from water by zeolite imidazolate skeleton(ZIF-67) *J. Funct. Mater.* 2020; Vol. *51* 2, p 6.
(26) Ablouh, E. H.; Kassab, Z.; Hassani, F.; et al. Phosphorylated cellulose paper as highly efficient adsorbent for cadmium heavy metal ion removal in aqueous solutions. *RSC Adv.* **2021**, *12* (2), 1084−1094.
(27) Ali, E. N. Removal of Heavy Metals from Water and Wastewater Using Moringa oleifera *Trace Metals in the Environment-New Approaches and Recent Advances* 2020; Vol. *23* 16, p 64.
(28) Guo, W. C.; Du, L. Y.; Liang, C. H.; Wu, Y.; Lin, D. S.; Zhang, X. F.; et al. Effects of Natural and Ammonium Chloride/Calcium Chloride-Modified Zeoliteson Cadmium Speciation in Contaminated Soil. *Chin. J. Soil Sci.* **2019**, *50* (719), 724.
(29) Wang, J.; Sun, M.Influencing factors of adsorption properties of modified zeolite by chitosan *Water Technol.* 2019; Vol. *13* 2, p 4.
(30) Du, L.; Xu, C.Study on solubility of chitosan *Chem. Eng.* 1990; Vol. *000* 006, pp 10−12.
(31) Song-lin, Z. A review of the control of pore texture of phosphoric acid-activated carbons. *New Carbon Mater.* **2018**, *33* (04), 289−302.
(32) Xiao, L.; Yang, C.; Liu, Z.; Kou, H.Preparation and photocatalytic performances of diatomite/Bi/g-C_3N_4 composite material *New Chem. Mater.* 2022; Vol. *50* 11, pp 130−135.
(33) Buapuean, T.; Jarudilokkul, S. Synthesis of Mesoporous Zn-doped TiO_2 Nanoparticles by Colloidal Emulsion Aphrons and Their Use for Dye-sensitized Solar Cells. *Russ. J. Appl. Chem.* **2020**, *93* (8), 1229−1236, DOI: 10.1134/S1070427220080169.
(34) Tan, D. J.; Pajarito, B. B. Assessment on the Synthesis and Performance of Low-Cost Chitosan-Coated Natural Zeolite Adsorbent for Post-Combustion Carbon Dioxide Capture. *Key Eng. Mater.* **2018**, *775*, 383−389.
(35) Jiang, T. Chitosan *Beijing: Chem. Ind. Press* 2006.
(36) Li, Y.; Shi, H.; Wu, C.; Liu, Z.; Gao, S.; Liu, G.et al.Review on adsorption of heavy metals in water by modified zeolite with cation surfactant *Water Purif. Technol.* 2020; Vol. *39* 12, pp 73−79.

https://doi.org/10.1021/acsomega.3c06041
ACS Omega 2024, 9, 573−584